# SATURATED-UNSATURATED FLOW TO A WELL WITH STORAGE IN A COMPRESSIBLE UNCONFINED AQUIFER

Phoolendra Kumar Mishra[1] and Shlomo P Neuman

Department of Hydrology and Water Resources

University of Arizona

Tucson, Arizona 85721

[1]Now with the Hydrology, Geochemistry and Geology Group at Los Alamos National Laboratory, MS T003, Los Alamos, NM 87545

## ABSTRACT

*Mishra and Neuman* [2010] developed an analytical solution for flow to a partially penetrating well of zero radius in a compressible unconfined aquifer that allows inferring its saturated and unsaturated hydraulic properties from responses recorded in the saturated and/or the unsaturated zone. Their solution accounts for horizontal as well as vertical flows in each zone. It represents unsaturated zone constitutive properties in a manner that is at once mathematically tractable and sufficiently flexible to provide much improved fits to standard constitutive models such as those of *Gardner* [1958] and *Russo* [1988], *Brooks and Corey* [1964] or *van Genuchten* [1980] and *Mualem* [1976]. In this paper we extend the solution of *Mishra and Neuman* [2010] to the case of a finite diameter pumping well with storage; investigate the effects of storage in the pumping well and delayed piezometer response on drawdowns in the saturated and unsaturated zones as functions of position and time; validate our solution against numerical simulations of drawdown in a synthetic aquifer having unsaturated properties described by the *van Genuchten* [1980] - *Mualem* [1976] model; use our solution to analyze 11 transducer-measured drawdown records from a seven-day pumping test conducted by University of Waterloo researchers at the Canadian Forces Base Borden in Ontario, Canada; validate our parameter estimates against manually-measured drawdown records in 14 other piezometers at Borden; and compare (a) our estimates of aquifer parameters with those obtained on the basis of all these records by *Moench* [2008], (b) on the basis of 11 transducer-measured drawdown records *by Endres et al.* [2007], (c) our estimates of van Genuchten - Mualem parameters with those obtained on the basis of laboratory drainage data from the site by *Akindunni and Gillham* [1992], and (d) our corresponding prediction of how effective saturation varies with elevation above the initial water table under static conditions with a profile based on water contents

measured in a neutron access tube at a radial distance of about 5 m from the center of the pumping well.

## INTRODUCTION

Drawdowns generated by extracting water from a large diameter (e.g. water supply) well in an unconfined aquifer are affected by wellbore storage. *Narasimhan and Zhu* [1993] used a numerical model to demonstrate that early time drawdown in an unconfined aquifer tends to be masked by wellbore storage effects. The same was confirmed analytically [*Moench*, 1997] and numerically [*Moench*, 2008] in the context of a seven-day pumping test conducted by University of Waterloo researchers at the Canadian Forces Base Borden in Ontario, Canada. Yet virtually all analytical solutions of flow to a well in an unconfined aquifer, other than that of *Moench* [1997], have considered the pumping well to have zero radius and, therefore, no capacity to store water; see recent reviews in *Tartakovsky and Neuman* [2007] and *Mishra and Neuman* [2010].

*Mishra and Neuman* [2010] developed an analytical solution for flow to a partially penetrating well of zero radius in a compressible unconfined aquifer that allows inferring its saturated and unsaturated hydraulic properties from drawdowns recorded in the saturated and/or the unsaturated zones. Their solution, like that of *Tartakovsky and Neuman* [2007], accounts for horizontal as well as vertical flows in both zones. It represents unsaturated zone constitutive properties in a manner that is at once mathematically tractable and sufficiently flexible to provide much improved fits to standard constitutive models such as those of *Gardner* [1958] and *Russo* [1988], *Brooks and Corey* [1964] or *van Genuchten* [1980] and *Mualem* [1976].

In this paper we extend the saturated-unsaturated solution of *Mishra and Neuman* [2010] to the case of a finite diameter pumping well with storage. We further account for delayed response of piezometers (and observation wells) due to their own ability to store water, based on a theory due to *Hvorslev* [1951] as done by *Neuman and Gardner* [1989] and *Moench* [1997]. We then investigate the effects of pumping well storage and delayed piezometer response on drawdowns in the saturated and unsaturated zones as functions of position and time; validate our solution against numerical simulations of drawdown in a synthetic aquifer having unsaturated properties described by the *van Genuchten* [1980] - *Mualem* [1976] model; use our solution to analyze a seven-day pumping test conducted by University of Waterloo researchers at the Canadian Forces Base Borden in Ontario, Canada; and compare our results with those obtained for this same aquifer by others.

## THEORY

### Statement of Problem

We consider a compressible unconfined aquifer of infinite lateral extent resting on an impermeable boundary (Figure 1). The aquifer is spatially uniform and anisotropic, with constant specific storage $S_s$ and fixed ratio $K_D = K_z / K_r$ between vertical and horizontal saturated hydraulic conductivities, $K_z$ and $K_r$, respectively. The aquifer is saturated beneath an initially horizontal water table at elevation $z = b$ defined as a $\psi = \psi_a$ isobar where $\psi$ is pressure head and $\psi_a \leq 0$ is the pressure head required for air to enter a saturated medium. A saturated capillary fringe at non-positive pressure $\psi_a \leq \psi \leq 0$ extends from the water table down to the $\psi = 0$ isobar (corresponding to the traditional definition of a water table) at elevation $b + \psi_a$ (note that the capillary fringe disappears if one sets $\psi_a = 0$). Prior to the onset of pumping the saturated and overlying unsaturated zones are at uniform initial hydraulic head $h_0 = b + \psi_a$. Starting at time $t$ = 0, water is withdrawn at a constant volumetric rate $Q$ from a well of finite radius $r_w$ and wellbore storage coefficient $C_w$ (volume of water released from storage in the pumping well per unit drawdown in this well). The pumping well penetrates the saturated zone between depths $l$ and $d$ below the initial water table (at air entry pressure).

Like *Mishra and Neuman* [2010] we represent the aquifer water retention curve by means of an exponential function

$$S_e = \frac{\theta(\psi) - \theta_r}{S_y} = e^{a_c(\psi - \psi_a)} \qquad\qquad a_c \geq 0 \qquad\qquad (1)$$

where $S_e$ is effective saturation, $\theta_r$ is residual water content and $S_y = \theta_s - \theta_r$ is drainable porosity or specific yield. Like them we adopt *Gardner's* [1958] exponential model for relative hydraulic conductivity,

$$k(\psi) = \begin{cases} e^{a_k(\psi - \psi_k)} & \psi \leq \psi_k \\ 1 & \psi < \psi_k \end{cases} \qquad\qquad a_k \geq 0, \qquad\qquad (2)$$

with parameters $a_k$ and $\psi_k$ that generally differ from $a_c$ and $\psi_a$ in (1). The parameter $\psi_k \leq 0$ represents a pressure head above which relative hydraulic conductivity is effectively equal to unity, which is sometimes but not always equal to the air entry pressure head $\psi_a$. In addition to being mathematically tractable, these exponential expressions are sufficiently flexible to provide acceptable (though not perfect) fits to standard constitutive models such as those mentioned earlier.

**Point Drawdown in Saturated and Unsaturated Zones**

*Mishra and Neuman* [2010] have shown that, when the pumping well has zero radius (and hence no capacity to store water), drawdown in the saturated zone can be expressed as

$$s = s_H + s_U \qquad\qquad (3)$$

where $s_H$ is *Hantush's* [1964] solution for flow to a partially penetrating well of zero radius in a confined aquifer and $s_U$ is a correction accounting for water table and unsaturated zone effects. Laplace transforms of $s_U$ and of drawdown $\sigma$ in the unsaturated zone are given by *Mishra and Neuman* [2010], respectively, as

$$\bar{s}_U(r_D, z_D, p_D) = -\int_0^\infty \frac{\cosh(\mu z_D)}{\cosh(\mu) - \frac{\mu}{q_D}\sinh(\mu)} \left(\bar{\bar{s}}_H\right)_{z_D=1} \frac{{r_D}^2 K_D}{r^2} y J_0\left[y K_D^{1/2} r_D\right] \mathrm{dy} \tag{4}$$

and

$$\bar{\sigma}(r_D, z_D, p_D) = \begin{cases} -\int_0^\infty e^{a_{kD}(z_D-1)/2}\left[1 - \frac{\cosh(\mu)}{\cosh(\mu) - \frac{\mu}{q_D}\sinh(\mu)}\right] \frac{J_\nu[i\phi(z_D-1)] + \chi Y_\nu[i\phi(z_D-1)]}{J_\nu[i\phi(0)] + \chi Y_\nu[i\phi(0)]} \\ \cdot\left(\bar{\bar{s}}_H\right)_{z_D=1} \frac{{r_D}^2 K_D}{r^2} y J_0\left[y K_D^{1/2} r_D\right] \mathrm{dy} \qquad \text{for } a_{cD} \neq a_{kD} \\ -\int_0^\infty \left[1 - \frac{\cosh(\mu)}{\cosh(\mu) - \frac{\mu}{q_D}\sinh(\mu)}\right] \frac{e^{\delta_{1D}(z_D-1)} + \chi e^{\delta_{2D}(z_D-1)}}{1+\chi} \\ \cdot\left(\bar{\bar{s}}_H\right)_{z_D=1} \frac{{r_D}^2 K_D}{r^2} y J_0\left[y K_D^{1/2} r_D\right] \mathrm{dy} \qquad \text{for } a_{cD} = a_{kD} = \kappa_D \end{cases} \tag{5}$$

where $r_D = r/b$, $z_D = z/b$, $\mu^2 = y^2 + \frac{p_D}{t_s K_D r_D^2}$, $t_s = \alpha_s t / r^2$, $\alpha_s = K_r / S_s$, $q_D = qb$, $a_{kD} = a_k b$,

$a_{cD} = a_c b$, $\phi(z_D) = \sqrt{\frac{4B_D}{{\lambda_D}^2} e^{\lambda_D z_D / 2}}$, $\lambda_D = a_{kD} - a_{cD}$, $B_D = p_D \frac{S_D a_{cD} e^{a_{kD}(\psi_{kD} - \psi_{aD})}}{t_s K_D r_D^2}$, $S_D = S_y / S$,

$\psi_{kD} = \psi_k / b$, $\psi_{aD} = \psi_a / b$, $\delta_{1D,2D} = \delta_{1,2} b = \frac{\kappa_D \mp \sqrt{{\kappa_D}^2 + 4\left(B_D + y^2\right)}}{2}$, $\nu = \sqrt{\frac{{a_{kD}}^2 + 4y^2}{{\lambda_D}^2}}$, and

$p_D = pt$ are dimensionless quantities, $p$ being the parameter of the Laplace transform;

$$\left(\bar{\bar{s}}_H\right)_{z_D=1} = -\frac{Qt}{2\pi T p_D} \frac{r^2}{{r_D}^2 K_D} \left\{ \frac{\sinh\left[\mu\left(1 - l_D\right)\right] - \sinh\left[\mu\left(1 - d_D\right)\right]}{\mu^2\left(l_D - d_D\right)\sinh(\mu)} \right\} \tag{6}$$

is the Lapalce and Hankel transformed version of $s_H$, $T = K_r b$ being transmissivity; and

$$
\chi = \begin{cases} -\dfrac{\left(a_{kD}+n\lambda_D\right)J_n\left[i\phi\left(L_D\right)\right]-2i\sqrt{B_D e^{\lambda_D L_D}}\,J_{n+1}\left[i\phi\left(L_D\right)\right]}{\left(a_{kD}+n\lambda_D\right)Y_n\left[i\phi\left(L_D\right)\right]-2i\sqrt{B_D e^{\lambda_D L_D}}\,Y_{n+1}\left[i\phi\left(L_D\right)\right]} & a_{kD}\neq a_{cD} \\ i & a_{kD}\neq a_{cD},\, L_D\to\infty \\ -\dfrac{\delta_{1D}}{\delta_{2D}}e^{\left(\delta_{1D}-\delta_{2D}\right)L_D} & a_{kD}=a_{cD} \\ 0 & a_{kD}=a_{cD},\, L_D\to\infty \end{cases} \tag{7}
$$

$$
qb = \begin{cases} \left(\dfrac{a_{kD}}{2}+\dfrac{n\lambda_D}{2}\right)-i\sqrt{B_D}\,\dfrac{J_{n+1}\left[i\phi(0)\right]+\chi Y_{n+1}\left[i\phi(0)\right]}{J_n\left[i\phi(0)\right]+\chi Y_n\left[i\phi(0)\right]} & a_{kD}\neq a_{cD} \\ \dfrac{\delta_{1D}+\chi\delta_{2D}}{1+\chi} & a_{kD}=a_{cD} \\ \delta_{1D} & a_{kD}=a_{cD},\ L_D\to\infty \end{cases} \tag{8}
$$

where $L_D = L/b$, $J_n$ and $Y_n$ being Bessel functions of first and second kind, respectively, of order $n$.

Let $s_C$ be a modified version of *Hantush's* [1964] confined aquifer solution, $s_H$, which accounts for storage in a partially penetrating pumping well of finite radius. We take this modified solution to satisfy the following equations:

$$
\frac{1}{r}\frac{\partial}{\partial r}\left(r\frac{\partial s_C}{\partial r}\right)+K_D\frac{\partial^2 s_C}{\partial z^2}=\frac{1}{\alpha_s}\frac{\partial s_C}{\partial t} \qquad r\geq r_w \qquad 0\leq z<b \tag{9}
$$

$$
s_C(r,z,0)=0 \qquad r\geq r_w \qquad 0\leq z<b \tag{10}
$$

$$
s_C\left(\infty,z,t\right)=0 \qquad 0\leq z<b \tag{11}
$$

$$
\frac{\partial s_C}{\partial z}=0 \qquad r\geq r_w \qquad z=0 \quad z=b \tag{12}
$$

$$
\left(\frac{\partial s_C}{\partial r}\right)_{r=r_w}=0 \qquad 0\leq z\leq b-l \qquad b-d\leq z\leq b \tag{13}
$$

$$2\pi K_r\left(l-d\right)r_w\left(\frac{\partial s_C}{\partial r}\right)_{r=r_w+}-C_W\left(\frac{\partial s_C}{\partial t}\right)_{r=r_w}=-Q \qquad b-l\le z\le b-d \tag{14}$$

$$s_C=\left(s_C\right)_{r=r_w} \qquad r\le r_w \qquad 0\le z<b \tag{15}$$

where $r=r_w+$ designates a radius exceeding $r_w$ by an infinitesimal amount. Equation (14) assumes as did *Hantush* [1964], *Dagan* [1967] and *Neuman* [1974] that horizontal flow into the pumping well is uniformly distributed along its screened interval (see *Zhan and Zlotnik* [2002] for a discussion of this assumption's validity); equation (15) is an approximation extending $s_C$ to $r\le r_w$ in order to render its domain of definition compatible with those of $s_U$ and $\sigma$. Whereas the first introduces a minor inaccuracy inside and near the pumping well, the second does so near the interface between the saturated and the unsaturated zones along the axis of the well. Both have minimal effects on the quality of the solution at some distance from the well axis, as we demonstrate through comparison with a numerical solution in a subsequent section.

The Laplace transformed solution of (9) - (15), whose development for $r_D\ge r_{wD}$ is detailed in Appendix A, takes the form

$$\bar{s}_C\left(r_D,z_D,p_D\right)=\begin{cases}C_0K_0\left(r_{wD}\phi_0\right)+\sum_{n=1}^{\infty}C_nK_0\left(r_{wD}\phi_n\right)\cos\left[n\pi\left(1-z_D\right)\right] & r_D\le r_{wD}\\ C_0K_0\left(r_D\phi_0\right)+\sum_{n=1}^{\infty}C_nK_0\left(r_D\phi_n\right)\cos\left[n\pi\left(1-z_D\right)\right] & r_D\ge r_{wD}\end{cases} \tag{16}$$

where

$$C_0=\frac{Q}{2\pi Tp_D}\frac{1}{r_{wD}\phi_0K_1\left(r_{wD}\phi_0\right)+\dfrac{C_{wD}}{2\left(l_D-d_D\right)}r_{wD}{}^2\left(\phi_0\right)^2K_0\left(r_{wD}\phi_0\right)},$$

$$C_n=\frac{Q}{4Tp_D\pi^2\left(l_D-d_d\right)n}\frac{\left[\sin\left(n\pi l_D\right)\text{-}\sin\left(n\pi d_D\right)\ \right]}{r_{wD}\phi_nK_1\left(r_{wD}\phi_n\right)+\dfrac{C_{wD}}{2\left(l_d-d_d\right)}r_{wD}{}^2\left(\phi_0\right)^2K_0\left(r_{wD}\phi_n\right)},$$

$C_{wD} = C_w / \left(\pi S_s b r_w{}^2\right)$ and $\phi_n = \sqrt{p_D / t_s + r_D{}^2 K_D n^2 \pi^2}$, $K_0$ and $K_1$ being modified Bessel functions of second kind and, respectively, orders zero and one. Appendix A also shows that the Hankel transform of (16), evaluated at $z_D = 1$, is

$$\left(\bar{\bar{s}}_C\right)_{z=b} = C_0 \frac{r^2}{K_D r_D^2} \left\{ \frac{y_D r_{wD}}{y^2} J_1\left(y_D r_{wD}\right) K_0\left(r_{wD}\phi_0\right) + \frac{r_{wD}\phi_0 J_0\left(y_D\right) K_1\left(\phi_0\right) - y_D r_{wD} J_1\left(y_D\right) K_0\left(\phi_0\right)}{\mu^2} \right\}$$
$$+ \sum_{n=1}^{\infty} C_n \frac{r^2}{K_D r_D^2} \left\{ \frac{y_D r_{wD}}{y^2} J_1\left(y_D r_{wD}\right) K_0\left(r_{wD}\phi_0\right) + \frac{r_{wD}\phi_n J_0\left(y_D\right) K_1\left(\phi_n\right) - y_D r_{wD} J_1\left(y_D\right) K_0\left(\phi_n\right)}{\mu^2 + n^2\pi^2} \right\} \tag{17}$$

where $y_D = y K_D^{1/2} r_D$, $J_0$ and $J_1$ being modified Bessel functions of first kind and, respectively, orders zero and one.

Replacing $s_H$ in (3) with $s_C$, the Laplace transform of which is given by (16), and $\left(\bar{\bar{s}}_H\right)_{z_D=1}$ in (4) - (5) with $\left(\bar{\bar{s}}_C\right)_{z_D=1}$ defined in (17), transforms the solution of *Mishra and Neuman* [2010] to one which accounts for the finite radius and storage capacity of the pumping well.

In the limit as $x \to 0$, $x K_1(x) \to 1$ and $x^2 K_0(x) \to 0$. Correspondingly, in the limit as $r_w \to 0$ one finds $s_C \to s_H$ and our solution reduces to that of *Mishra and Neuman* [2010].

The time domain equivalents $s_c$, $s_U$ and $\sigma$ of $\bar{s}_c$, $\bar{s}_U$ and $\bar{\sigma}$ are obtained through numerical Laplace transform inversion using an algorithm due to *Crump* [1976] as modified by *de Hoog et. al.* [1982]. Whereas standard inversion with respect to *p* is done over a time interval [0,t] , we do the inversion with respect to $p_D$ over a unit dimensionless time (corresponding to $p_D{}^{-1}$) interval [0,1], regardless of what $t_s$ is.

## Vertically Averaged Drawdown in Observation Well

Drawdown in an observation well that penetrates the saturated zone between elevations $z_{D1} = z_1 / b$ and $z_{D2} = z_2 / b$ (Figure 1) is obtained by averaging the point drawdown over this interval according to

$$s_{z_{D2}-z_{D1}}(r_D, t_s) = \frac{1}{z_{D2} - z_{D1}} \int_{z_{D1}}^{z_{D2}} s\left(r_D, z_D, t_s\right) dz_D . \tag{18}$$

## Delayed Piezometer or Observation Well Response

When water level is measured in a piezometer or observation well having storage coefficient $C$ the response of the measuring instrument is delayed in time. In a manner analogous to *Hvorslev* [1951] and *Neuman and Gardner* [1989] we write

$$s = s_m + t_B \frac{\partial s_m}{dt} \tag{19}$$

where $s$ is actual drawdown, $s_m$ is measured (delayed) drawdown, $t_B = \dfrac{C}{FK}$ is basic (characteristic) time lag of the instrument, $F$ is a shape factor (having dimensions of length) and $K$ is hydraulic conductivity of the formation or of a skin, if such is present. The characteristic time lag $t_B$ can be determined by means of a slug or pulse test, obviating the need to know $C$, $F$ or $K$. Integrating (19) allows expressing $s_m$ in terms of $s$ via

$$s_m = s\left[1 - e^{-t/t_B}\right] \tag{20}$$

or its dimensionless equivalent [*Neuman and Gardner*, 1989]

$$s_{mD} = s_D\left[1 - e^{-t_s/t_{Bs}}\right] \tag{21}$$

where $t_{Bs} = \dfrac{\alpha_s t_B}{r^2}$.

## EFFECTS OF PUMPING WELL AND OBSERVATIONAL DELAY ON DRAWDOWN

We illustrate the impacts of pumping well and piezometer (or observation well) storage on drawdown for the case where $K_D = 1$, $S_s b / S_y = 1/100$, $a_{kD} = a_{cD} = 10$, $\psi_{aD} = \psi_{kD}$, $d_D = 0.0$, $l_D = 0.5$ and $r_w / b = 0.02$. Point drawdowns in the saturated zone are examined at $r_D = 0.2$ and $z_D = 0.5$.

### Dimensionless time-drawdown in pumping well

We start by considering drawdown in a pumping well with storage. Figure 2 compares variations in dimensionless drawdown $s_D\left(r_D, z_D, t_s\right) = \left(4\pi K_r b / Q\right) s\left(r_D, z_D, t_s\right)$ with dimensionless time $t_s = \alpha_s t / r^2$ in a pumping well having dimensionless storage coefficient $C_{wD} = 1.0 \times 10^2$ predicted by our solution $s_D = s_{CD} + s_{UD}$, its confined component $s_{CD}$, the solution of *Mishra and Neuman* [2010] and that of *Hantush* [1964]. At early dimensionless time both $s_D = s_{CD} + s_{UD}$ and $s_{CD}$ vary linearly with $t_s$, implying that water is derived entirely from storage in the pumping well. Solutions due to *Mishra and Neuman* [2010] and *Hantush* [1964], which disregard pumping well storage, predict a much earlier and steeper rise in drawdown. As dimensionless time increases, the effects of finite radius and wellbore storage dissipate, and our solution approaches asymptotically that of *Mishra and Neuman* [2010]. The confined component of our solution, $s_{CD}$, approaches asymptotically that of *Hantush* [1964]. Both unconfined solutions fall below the two confined solutions at late dimensionless time due to gravity drainage at and above the water table.

Figure 3 shows how dimensionless time-drawdown variations in the pumping well are affected by the wellbore storage coefficient $C_{wD}$. Consistent with the solution of *Papadopulos and Cooper* [1967] for a fully penetrating well in a confined aquifer, the larger is $C_{wD}$ the longer does wellbore storage impact drawdown in the pumping well. As $C_{wD}$ diminishes our early time solution approaches that of *Yang et.al* [2006] for a partially penetrating well of finite radius, but no storage, in a confined aquifer. The latter solution in turn approaches that of *Hantush* [1964] asymptotically with time. Our new solution approaches asymptotically that of *Mishra and Neuman* [2010] with time, both falling below the two confined solutions at late dimensionless time.

**Dimensionless time-drawdown in saturated zone piezometer without delay**

Figure 4 depicts dimensionless time-drawdown variations at dimensionless radial distance $r_D = 0.2$ from the axis of the pumping well and dimensionless elevation $z_D = 0.5$ in the saturated zone for different values of $C_{wD}$. When $C_{wD}$ is large, the early dimensionless time-drawdown curve exhibits a slope of close to 1 on log-log scale, reflecting a pronounced effect of pumping well storage on early drawdown in a nearby piezometer. As $C_{wD}$ decreases this effect diminishes, the early time-drawdown curves grow steeper, approaching asymptotically the solutions of *Mishra and Neuman* [2010] and *Hantush* [1964] as $C_{wD}$ tends to zero. At late time the drawdown tends asymptotically to the solution of *Mishra and Neuman* [2010] regardless of $C_{wD}$.

**Dimensionless time-drawdown in saturated zone piezometer with storage**

Figure 5 illustrates the impact of dimensionless piezometer time lag $t_{Bs}$ on dimensionless time-drawdown at $r_D = 0.2$ and $z_D = 0.5$ in the saturated zone when the pumping well lacks storage. The effect is qualitatively similar to that of pumping well storage in Figure 4.

**Dimensionless time-drawdown in unsaturated zone**

Figure 6 depicts dimensionless time-drawdown variations at dimensionless radial distance $r_D = 0.2$ and dimensionless elevation $z_D = 1.25$ in the unsaturated zone for different values of $C_{wD}$. A comparison of Figure 6 with Figure 4 reveals that pumping well storage has a much lesser impact on drawdown in the unsaturated zone than in the saturated zone. Regardless of $C_{wD}$ drawdown in the unsaturated zone increases at a rate that varies monotonically with time, in contrast to the saturated zone in which this rate exhibits an S-shape inflection characteristic of delayed response.

## SYNTHETIC AQUIFER TEST

To evaluate the ability of our analytical solution to reproduce drawdowns under less restrictive conditions than those we have used to derive it, we compare it with drawdowns simulated numerically by the STOMP code [*White et al.*, 2000]. We simulate flow in an isotropic aquifer $(K_D = 1.0)$ with horizontal hydraulic conductivity $K_r = 1.0 \times 10^{-4}\ m/s$, specific storage $S_s = 4.0 \times 10^{-5}\ m^{-1}$ and specific yield $S_y = 0.322$. In the numerical model, water retention and relative hydraulic conductivity are described by the constitutive model of *van Genuchten* [1980] and *Mualem* [1976] with parameters $\log \alpha = -1.453$, $\theta_s = 0.375$, $\theta_r = 0.053$ and $\log n = 0.502$ typical of sandy soils [*Schaap et al.,* 2001]. In our analytical solution we set $\psi_a = 14.2\ \text{cm}$, $\psi_k = 8.3\ \text{cm}$, $a_k = 8.2\ \text{m}^{-1}$ and $a_c = 3.4\ \text{m}^{-1}$, values estimated by *Mishra and Neuman* [2010, Figure A3] upon fitting (1) and (2) by least squares to the van Genuchten - Mualem model with the above parameters. The saturated-unsaturated aquifer rests on an impermeable horizontal boundary, has a combined thickness of 9 m and a water table (defined here as a zero-pressure isobar) located initially 2.75 m below its horizontal land surface boundary. The pumping well has an inner diameter of 0.13 m, penetrates the bottom 3.65 m of the aquifer and discharges at a rate of 40 l/min. We simulate it as a highly permeable medium with specific storage 100 times larger than that of the aquifer, yielding a dimensionless wellbore storage coefficient of $C_{wD} = 58.2$.

Figure 7 compares time-drawdowns predicted analytically and simulated numerically at three radial distances $r$ = 0.26, 0.80 and 1.51 m from the axis of the pumping well at elevation $z = 2.0$ m above the aquifer bottom in the saturated zone. The agreement is acceptable at all three points, at all times, being least satisfactory at intermediate times but tending to improve as radial distance and time increase.

Figure 8 compares time-drawdowns at radial distance $r = 1.51\ m$ and elevation $z = 2.0\ m$ in the saturated zone obtained (1) analytically with our solution and numerically with STOMP upon considering pumping well storage but ignoring delayed piezometer response or, more specifically, upon setting $C_{wD} = 58.2$ and $t_b$ = 0 min, and (2) analytically with the solution of *Mishra and Neuman* [2010] which ignores pumping well storage, but considering delayed piezometer response by setting $t_b$ = 0.011 min. Figure 8 makes clear that the two cases are difficult to distinguish from each other, i.e., that it may be hard to differentiate between the effects of pumping well and piezometer storage based solely on observed drawdowns. Correspondingly, it may be difficult to estimate the corresponding storage parameters simultaneously on the basis of drawdown data alone.

Figure 9 compares time-drawdowns predicted analytically and simulated numerically at three radial distances $r$ = 1.51, 5.04 and 10.71 m from the axis of the pumping well at elevation $z = 6.61$ m in unsaturated zone. The agreement is less good than in the saturated zone but acceptable at all three points, tending to improve as radial distance and time increase.

## ANALYSIS OF BORDEN AQUIFER TEST

A 7-day pumping test was conducted during August 2001 by University of Waterloo researchers at the Canadian Forces Base Borden in Ontario, Canada. Details of the test are described by *Bevan et al.* [2005]. At the test site the aquifer is approximately 9.0 *m* thick, consists largely of unconsolidated medium-grain sand of glacio-deltaic or glacio-fluvial origin and overlies a clayey silt aquitard of relatively low permeability. A well screened between depths 2.6 and 6.25 m below the initial water table, located 2.75 m below the land surface, was pumped at a constant rate of 40 l/min for 7 days. Hydraulic head variations were monitored in 25 piezometers installed at diverse locations, distances and depths around the pumping well (Figures 10 and 11). As indicated in Figure 11, head variations in 11 piezometers and in the pumping well were measured by means of pressure transducers connected to data loggers. These 11 records, spanning a time interval from 2 seconds to 10,457 minutes, were fitted by us simultaneously to our analytical solution by least squares using the parameter estimation code PEST [*Doherty*, 2004]. Similar to *Moench* [2008], we specified the characteristic time lag $t_B$ of each piezometer *a priori* by setting $C = \pi r_p^2$, $K = K_r$ and $F = 2\pi L_p / \left[ L_p / 2r_r + \sqrt{1 + \left( L_p / 2r_r \right)^2} \right]$ where $L_p$ and $r_p$ are the screen length and radius, respectively, of any piezometer [*Hvorslev*, 1951]. The results of the fit are illustrated in Figure 12 and listed, together with corresponding 95% confidence intervals, in Table 1. Table 2 compares our parameter estimates with those obtained by *Endres et.al.* [2007] on the basis of 11 transducer-measured drawdown records and by *Moench* [2008] on the basis of drawdowns recorded in all 25 piezometers. Whereas our estimates of hydraulic conductivity and specific storage are similar to those obtained by *Endres et.al.* [2007] and *Moench* [2008], our estimate

0.301 of specific yield is somewhat higher than the value 0.284 obtained by *Endres et.al.* [2007] but significantly higher than the value 0.25 arbitrarily assigned to the aquifer by *Moench* [2008]. Our estimate of specific yield is virtually identical with the value 0.30 reported by *Nwankwor et al.* [1984] on the basis of laboratory drainage experiments on samples of aquifer material from the site.

Our estimates of exponential constitutive model parameters $a_c = 5.68\ m^{-1}$, $a_k = 23.66\ m^{-1}$ and $\psi_a - \psi_k = 3.12\ cm$ in Table 2 provide a least squares fit to *van Genuchten* [1980] – *Mualem* [1976] model parameters $\psi_a = 34.1\ cm$, $\psi_k = 30.98\ cm$, $\alpha = 2.32\ m^{-1}$ and $n = 5.85$. The corresponding exponential and van Genuchten - Mualem functions are plotted in Figure 13. Our pumping test estimate $\alpha = 2.32\ m^{-1}$ is somewhat larger and our $n = 5.85$ smaller than values $\alpha = 1.9\ m^{-1}$ and $n = 6.095$ obtained by *Akindunni and Gillham* [1992, Table 1] on the basis of laboratory drainage data from the site. Effective saturation values based on measured water contents above the water table in neutron access tube MBN − 5, located at a radial distance of about 5 m from the center of the pumping well, are seen in Figure 13 to lie very close to our pumping test derived effective saturation curve (recall that, under static initial conditions, capillary pressure head is equivalent to elevation above the zero pressure isobar).

Finally we compare in Figure 14 drawdowns measured manually in 14 piezometers (shown by solid rectangles in Figure 11) with those predicted by our analytical solution with parameter estimates in Table 2 (based on transducer measurements in 11 other piezometers). The fit in all piezometers is fairly good. The fits in piezometers P13 and P16, located near the bottom of the aquifer (6.1 m below the initial water table), are less good due likely to the non-ideal nature of this boundary.

## CONCLUSIONS

Our work leads to following major conclusions:

1. A new analytical solution was developed for axially symmetric saturated-unsaturated flow in three dimensions to a well with storage that partially penetrates the saturated zone of a compressible vertically-anisotropic unconfined aquifer. The solution allows considering delayed response of piezometers and observation wells due to water storage in these measuring devices.
2. Our analytical solution agrees with numerical simulations of drawdown in both the saturated and the unsaturated zones of a synthetic aquifer having unsaturated properties described by the *van Genuchten* [1980] - *Mualem* [1976] constitutive model. Agreement between the two solutions in the saturated zone is closer than in the unsaturated zone, least satisfactory at intermediate times but tending to improve as radial distance and time increase.
3. The analytical solution demonstrates (and our numerical simulations confirm) that (a) pumping well storage may impact drawdowns at some horizontal and/or vertical distance from this well in the saturated zone as well as, though to a much lesser extent, in the unsaturated zone; (b) the effect of pumping well storage on drawdown in a piezometer (or observation well) is qualitatively similar, and therefore difficult to distinguish from, that of delayed piezometer response; (c) therefore, it may be difficult to estimate the corresponding storage parameters simultaneously on the basis of drawdown data alone; and (d) regardless of wellbore or piezometer storage, a log-log plot of drawdown versus time exhibits an S-shape inflection characteristic of delayed response in the saturated zone but not in the unsaturated zone.

4. We used our solution to analyze 11 transducer-measured drawdown records from a seven-day pumping test conducted by University of Waterloo researchers at the Canadian Forces Base Borden in Ontario, Canada, and to validate our parameter estimates against manually-measured drawdown records in 14 other piezometers at the site. The validation was satisfactory except in two piezometers near the aquifer bottom due likely to the non-ideal nature of this boundary.
5. Similar to *Moench* [2008], we specified the characteristic time lag of each Borden piezometer *a priori* based on its radius and screen length. Our estimates of hydraulic conductivity and specific storage are similar to those obtained on the basis of 11 transducer-measured records by *Endres et.al.* [2007] and all 25 drawdown records by *Moench* [2008]. Our estimate 0.301 of specific yield is somewhat higher than the 0.284 value obtained by *Endres et.al.* [2007] but significantly higher than the 0.25 value assigned to the aquifer by *Moench* [2008]. Our estimate of specific yield is virtually identical to the 0.30 value reported by *Nwankwor et al.* [1984] on the basis of laboratory drainage experiments on samples of aquifer material from the site.
6. Estimates of exponential constitutive model parameters entering into our analytical solution provide a least squares fit to the *van Genuchten* [1980] – *Mualem* [1976] model with parameters $\psi_a = 34.1\ cm$, $\psi_k = 30.98\ cm$, $\alpha = 2.32\ m^{-1}$ and $n = 5.85$. Our pumping test estimate $\alpha = 2.32\ m^{-1}$ is somewhat larger and our $n = 5.85$ smaller than values $\alpha = 1.9\ m^{-1}$ and $n = 6.095$ obtained by *Akindunni and Gillham* [1992, Table 1] on the basis of laboratory drainage data from the site.

7. Effective saturation values based on measured water contents above the water table in a neutron access tube located at a radial distance of about 5 m from the center of the pumping well lie very close to our pumping test derived effective saturation curve.

## APPENDIX A: LAPLACE AND LAPLACE-HANKEL TRANFORMS OF SATURATED ZONE SOLUTION

Introducing a new variable $r' = r\left(K_z / K_r\right)^{1/2} = rK_D{}^{1/2}$ and taking Laplace transform of (9) – (14) gives, for $r' \geq r_w{}'$,

$$\frac{\partial^2 \overline{s}_C}{\partial r'^2} + \frac{1}{r'}\frac{\partial \overline{s}_C}{\partial r'} + \frac{\partial^2 \overline{s}_C}{\partial z^2} = \frac{S_s}{K_z} p\overline{s}_C \qquad 0 \leq z \leq b \tag{A1}$$

subject to

$$\overline{s}_C\left(\infty, z, p\right) = 0 \qquad 0 \leq z \leq b \tag{A2}$$

$$\frac{\partial \overline{s}_C}{\partial z} = 0 \qquad z = 0 \quad z = b \tag{A3}$$

$$r_w'\left(\frac{\partial \overline{s}_C}{\partial r'}\right)_{r'=r_w'} = 0 \qquad 0 \leq z \leq b - l \qquad b - d \leq z \leq b \tag{A4}$$

$$2\pi K_r\left(l - d\right)r_w'\left(\frac{\partial \overline{s}_C}{\partial r'}\right)_{r'=r_w'} - C_w p\left(\overline{s}_C\right)_{r'=r_w'} = -\frac{Q}{p} \qquad b - l \leq z \leq b - d \tag{A5}$$

Defining the Fourier cosine transform of $\overline{s}_C\left(r', z, p\right)$ as [*Churchill*, 1958, pp. 354-355]

$$f_{\cos}\left[\overline{s}_{Cf}\left(r', z, p\right)\right] = \overline{s}_{Cf}\left(r', n, p\right) = \int_0^b \overline{s}_C\left(r', z, p\right)\cos\left(n\pi z / b\right)\,\mathrm{d}z \qquad n = 0,1,2,... \tag{A6}$$

with inverse

$$\overline{s}_C\left(r', z, p\right) = \frac{1}{b}\overline{s}_{Cf}\left(r', 0, p\right) + \frac{2}{b}\sum_{n=1}^{\infty}\overline{s}_{Cf}\left(r', n, p\right)\cos\left(n\pi z / b\right) \tag{A7}$$

implies that, by virtue of (A3),

$$f_{\cos}\left(\frac{\partial^2 \overline{s}_C}{\partial z^2}\right) = -\left(\frac{n\pi}{b}\right)^2 \overline{s}_{Cf}\left(r', n, p\right). \tag{A8}$$

Hence the Fourier cosine transformation of (A1) – (A5) leads to

$$\frac{\partial^2 \overline{s}_{Cf}}{\partial r'^2} + \frac{1}{r'}\frac{\partial \overline{s}_{Cf}}{\partial r'} - \left[\frac{p}{K_z / S_s} + \left(\frac{n\pi}{b}\right)^2\right]\overline{s}_{Cf} = 0 \tag{A9}$$

$$\overline{s}_{Cf}\left(\infty, n, p\right) = 0 \tag{A10}$$

$$r'_w\left(\frac{\partial \overline{s}_{Cf}}{\partial r'}\right)_{r'=r'_w} = 0 \tag{A11}$$

$$\begin{aligned} 2\pi K_r\left(l-d\right) r'_w\left(\frac{\partial \overline{s}_{Cf}}{\partial r}\right)_{r'=r_w'} - pC_w\left(\overline{s}_{Cf}\right)_{r'=r_w'} &= -\frac{Q}{p}\int_{b-l}^{b-d} \cos\left(n\pi z / b\right) dz \\ &= -\frac{Q}{p}\left(b / n\pi\right)\left[\sin\left\{n\pi\left(1-d/b\right)\right\} \text{-} \sin\left\{n\pi\left(1-l/b\right)\right\}\right] \end{aligned} \tag{A12}$$

The general solution of (A9) is

$$\overline{s}_{Cf} = AK_0\left(N'r'\right) + BI_0\left(N'r'\right) \tag{A13}$$

where $N'^2 = \dfrac{p}{K_z / S_s} + \left(n\pi / b\right)^2$, $I_0$ and $K_0$ being modified Bessel functions of first and second kind, respectively, of zero order. By virtue of (A10) $B = 0$. Substituting this and (A13) into (A12), noting that $\partial K_0\left(N'r'\right) / \partial r' = -N'K_1\left(N'r'\right)$, solving for *A* and substituting back into (A13) yields

$$\overline{s}_{Cf} = \frac{Q}{p}\frac{\left(b / n\pi\right)\left\{\sin\left[n\pi\left(1-d/b\right)\right] \text{-} \sin\left[n\pi\left(1-l/b\right)\right]\right\}}{2\pi K_r\left(l-d\right) N'r'_w K_1\left(N'r'_w\right) + p\, C_w K_0\left(N'r'_w\right)} K_0\left(N'r'\right). \tag{A14}$$

Noting that $\lim\limits_{n\to 0}\left[(1-d)\dfrac{\sin\left\{n\pi\left(1-d/b\right)\right\}}{\left\{n\pi\left(1-d/b\right)\right\}} - (1-l)\dfrac{\sin\left\{n\pi\left(1-l/b\right)\right\}}{\left\{n\pi\left(1-l/b\right)\right\}}\right] = l-d$ one obtains

$$\overline{s}_{Cf}\left(0\right)=\frac{Q}{p}\frac{K_0\left(r'\sqrt{\dfrac{p}{K_z/S_s}}\right)}{2\pi K_r r'_w\sqrt{\dfrac{p}{K_z/S_s}}K_1\left(r'_w\sqrt{\dfrac{p}{K_z/S_s}}\right)+\dfrac{pC_w}{\left(l-d\right)}K_0\left(r'_w\sqrt{\dfrac{p}{K_z/S_s}}\right)}. \tag{A15}$$

With this and (A7) the inverse Fourier cosine transform of (A14) can be written as

$$\begin{aligned}\overline{s}_C=&\frac{1}{b}\frac{Q}{K_r p}\frac{K_0\left(r'\sqrt{\dfrac{p}{K_z/S_s}}\right)}{2\pi r'_w\sqrt{\dfrac{p}{K_z/S_s}}K_1\left(r'_w\sqrt{\dfrac{p}{K_z/S_s}}\right)+\dfrac{pC_w}{K_r\left(l-d\right)}K_0\left(r'_w\sqrt{\dfrac{p}{K_z/S_s}}\right)}\\&+\frac{2}{b}\frac{Q}{K_r p}\sum_{n=1}^{\infty}\frac{\left(b/n\pi\right)\left[\sin\left(n\pi l/b\right)-\sin\left(n\pi d/b\right)\right]}{2\pi\left(l-d\right)N'r'_wK_1\left(N'r'_w\right)+\dfrac{pC_w}{K_r}K_0\left(N'r'_w\right)}\cos\left[n\pi\left(1-z/b\right)\right]K_0\left(N'r'\right)\end{aligned}. \tag{A16}$$

Recalling that $r'=rK_D^{1/2}$ allows reformulating this as

$$\begin{aligned}\overline{s}_C=&\frac{1}{b}\frac{Q}{K_r p}\frac{K_0\left(r\sqrt{\dfrac{p}{K_r/S_s}}\right)}{2\pi r_w\sqrt{\dfrac{p}{K_r/S_s}}K_1\left(r_w\sqrt{\dfrac{p}{K_r/S_s}}\right)+\dfrac{pC_w}{K_r\left(l-d\right)}K_0\left(r_w\sqrt{\dfrac{p}{K_r/S_s}}\right)}\\&+\frac{2}{b}\frac{Q}{K_r p}\sum_{n=1}^{\infty}\frac{\left(b/n\pi\right)\left[\sin\left(n\pi l/b\right)-\sin\left(n\pi d/b\right)\right]}{2\pi\left(l-d\right)Nr_wK_1\left(Nr_w\right)+\dfrac{pC_w}{K_r}K_0\left(Nr_w\right)}\cos\left[n\pi\left(1-z/b\right)\right]K_0\left(Nr\right)\end{aligned}. \tag{A17}$$

where $N^2=\dfrac{p}{K_r/S_s}+K_D\left(\dfrac{n\pi}{b}\right)^2$. Rewriting (A17) in dimensionless form yields (16).

The Hankel transform $\overline{\overline{s}}_C\left(a,z_D,p_D\right)$ of $\overline{s}_C\left(r,z_D,p_D\right)$ is

$$\begin{aligned}\overline{\overline{s}}_C\left(a,z_D,p_D\right)&=\int_0^{\infty}rJ_o(ar)\overline{s}_C\left(r,z_D,p_D\right)dr\\&=\left(\overline{s}_C\right)_{r=r_w}\int_0^{r_w}rJ_o(ar)dr+\int_{r_w}^{\infty}rJ_o(ar)\left\{C_0K_0\left(r\tau_0\right)+\sum_{n=1}^{\infty}C_nK_0\left(r\tau_n\right)\cos\left[n\pi\left(1-z_D\right)\right]\right\}dr\end{aligned} \tag{A18}$$

where $a$ is a parameter and $J_0$ is zero-order Bessel function of the first kind. Now [*Gradshteyn and Ryzhik*, 2008, pp. 630 and 665]

$$\int J_o(r)dr = rJ_1\left(r\right), \tag{A19}$$

$$\int_0^{r_w} rK_0\left(r\tau\right)J_o(ar)dr = \frac{1}{a^2+\tau^2}\left\{1+ar_wJ_1\left(ar\right)K_0\left(r\tau\right)-\tau r_wJ_0\left(ar\right)K_1\left(r\tau\right)\right\}, \tag{A20}$$

$$\int_0^{\infty} rK_0\left(r\tau\right)J_o(ar)dr = \frac{1}{a^2+\tau^2}. \tag{A21}$$

From (A20) and (A21) it follows that

$$\int_{r_w}^{\infty} rK_0\left(r\tau\right)J_o(ar)dr = \frac{\tau r_wJ_0\left(ar\right)K_1\left(r\tau\right)-ar_wJ_1\left(ar\right)K_0\left(r\tau\right)}{a^2+\tau^2}. \tag{A22}$$

This and (A19) allow expressing (A18) as

$$\begin{aligned}\overline{\overline{s}}_C\left(a,z_D,p_D\right) &= C_0\left\{\frac{r_w}{a}J_1\left(ar_w\right)K_0\left(r_w\tau_0\right)+\frac{\tau_0r_wJ_0\left(ar\right)K_1\left(r\tau_0\right)-ar_wJ_1\left(ar\right)K_0\left(r\tau_0\right)}{a^2+\tau_0{}^2}\right\}\\ &+\sum_{n=1}^{\infty}C_n\left\{\frac{r_w}{a}J_1\left(ar_w\right)K_0\left(r_w\tau_0\right)+\frac{\tau_nr_wJ_0\left(ar\right)K_1\left(r\tau_n\right)-ar_wJ_1\left(ar\right)K_0\left(r\tau_n\right)}{a^2+\tau_n{}^2}\right\}\cos\left[n\pi\left(1-z_D\right)\right]\end{aligned} \tag{A25}$$

Substituting $z_D = 1$ and defining a new variable $y = ar / K_D^{1/2}r_D$ transforms (A25) into (17).


## ACKNOWLEDGMENTS

This research was supported in part through a contract with Vanderbilt University under the Consortium of Risk Evaluation with Stakeholder Participation (CRESP) III, funded by the U.S. Department of Energy.

## REFERENCES


Akindunni, F. F. and Gillham, R. W. (1992), Unsaturated and Saturated Flow in Response to pumping of an Unconfined Aquifer: Numerical Investigation of Delayed Drainage. Ground Water, 30: 873–884. doi: 10.1111/j.1745-6584.

Bevan, M. J., A. L. Endres, D. L. Rudolph, and G. Parkin (2005), A field scale study of pumping-induced drainage and recovery in an unconfined aquifer, *J. Hydrol.*, *315*, 52–70, doi:10.1016/j.jhydrol.2005.04.006.

Brooks, R.H. and A.T. Corey (1964), Hydraulic properties of porous media, *Hydrol. Pap*. 30, Colo. State Univ., Fort Collins.

Churchill, R.V. (1958), *Operational Mathematics*, McGraw Hill, New York.

Crump, K. S. (1976), Numerical inversion of Laplace transforms using a Fourier series, *J. ACM* 23, pp. 89–96.

de Hoog, F. R., J. H. Knight, and A. N. Stokes (1982), An improved method for numerical inversion of Laplace transforms, *SIAM J. Sci. Stat. Comput.*, *3*, 357–366.

Dagan, G., A method of determining the permeability and effective porosity of unconfined anisotropic aquifers, Water Resour. Res., 3(4), 1059-1071, 1967.

Doherty, John, 1994, PEST-model-independent parameter estimation: Corinda, Australia, Watermark Computing, 122p.

Endres, A.L., J.P. Jones, and E.A. Bertrand (2007), Pumping-induced vadose zone drainage and storage in an unconfined aquifer: A comparison of analytical model predictions and field measurements, *Journal of Hydrology*, 335(1-2), 207-218, DOI: 10.1016/j.jhydrol.2006.07.018.

Gardner, W.R. (1958), Some steady state solutions of unsaturated moisture flow equations with application to evaporation from a water table, *Soil Sci.*, *85*, 228–232.

Gradshtein I.S. and I.M. Ryzhik (2008)**,** Tables of integrals series and products, *seventh edition*, Academic Press, New York.

Hantush, M. S. (1964), Hydraulics of wells, *Adv. Hydrosci.*, *1,* 281–442.

Hvorslev, M.J. (1951), Time lag and soil permeability in groundwater observations, U.S. Army Corps Engrs. Waterways Exp. Sta., Vicksburg, Miss. Bull. 36.

Mishra, P. K., and S. P. Neuman (2010), Improved forward and inverse analyses of saturated-unsaturated flow toward a well in a compressible unconfined aquifer, Water Resour. Res., 46, W07508, doi:10.1029/2009WR008899.

Moench, A.F. (1997), Flow to a Well of Finite Diameter in a Homogeneous, Anisotropic Water Table Aquifer, Water Resour. Res., 33(6), 1397-1407.

Moench, A. F. (2008), Analytical and numerical analyses of an unconfined aquifer test considering unsaturated zone characteristics, *Water Resour. Res.*, *44*, W06409, doi:10.1029/2006WR005736.

Mualem, Y. (1976), A new model for predicting the hydraulic conductivity of unsaturated porous media. *Water Resour. Res.*, 12, 513-522.

Narasimhan, T. N., and M. Zhu (1993), Transient flow of water to a well in an unconfined aquifer: Applicability of some conceptual models, *Water Resour. Res.*, *29*(1), 179–191, doi:10.1029/92WR01959.

Neuman, S. P. **(**1974**),** Effects of partial penetration on flow in unconfined aquifers considering Delayed aquifer response, *Water Resour. Res.*, *10,* 303–312, doi:10.1029/WR010i002p00303.

Neuman, S.P. and D.A. Gardner (1989), Determination of Aquitard/Aquiclude Hydraulic Properties From Arbitrary Water Level Fluctuations by Deconvolution, *Ground Water*, 27(1), 66-76.

Nwankwor, G.I., J.A. Cherry, and R.W. Gillham, A comparative study of specific yield determination for a shallow sand aquifer, *Ground Water*, 22(3), 303-312, 1984.

Papadopulos, I. S., and H. H. Cooper Jr. (1967), Drawdown in a well of large diameter, *Water Resour. Res.*, *3*(1), 241–244.

Russo, D. (1988), Determining soil hydraulic properties by parameter estimation: On the selection of a model for the hydraulic properties, *Water Resour. Res.*, 24(3) , 453 – 459.

Schaap, M.G., F.J. Leij, and M. Th. van Genuchten, (2001), Rosetta: a computer program for estimating soil hydraulic parameters with hierarchical pedotransfer functions. *Journal of Hydrology*, 251:163-176.

Tartakovsky, G. D., and S. P. Neuman (2007), Three-dimensional saturated-unsaturated flow with axial symmetry to a partially penetrating well in a compressible unconfined aquifer, *water Resour. Res.*, *43*, W01410, doi:10.1029/2006WR005153.

van Genuchten, M. T. (1980), A closed-form equation for predicting the hydraulic conductivity of unsaturated soils, *Soil Sci. Soc. Am. J.*, *44*, 892–898.

White, M.D., and M. Oostrom (2000), STOMP Subsurface Transport Over Multiple Phase: Theory Guid**e** PNNL-11216 (UC-2010), Pacific Northwest National Laboratory, Richland, Washington.

Yang, S.-Y., H.-D. Yeh, and P.-Y. Chiu (2006), A closed form solution for constant flux pumping in a well under partial penetration condition, *Water Resour. Res.*, 42, W05502, doi:10.1029/2004WR003889.

Zhan, H. and V.A. Zlotnik (2002), Ground water flow to horizontal or slanted wells in water table aquifers, *Water Resour. Res.*, 38(7), 1108, 10.1029/2001WR000401.

## TABLES

Table 1: Parameter estimates and their 95 % confidence limits obtained by fitting our solution to 11 transducer-measured drawdown records from Borden piezometers shown by open circles in Figure 11.

| Parameters | Estimated Value | 95 % Confidence Limits | |
|---|---|---|---|
| | | Lower | Upper |
| $K_r \ (m/s)$ | $6.36 \times 10^{-5}$ | $3.91 \times 10^{-5}$ | $7.13 \times 10^{-5}$ |
| $K_z / K_r$ | 0.45 | 0.37 | 0.56 |
| $S_s \ (m^{-1})$ | $5.67 \times 10^{-5}$ | $7.63 \times 10^{-6}$ | $2.44 \times 10^{-4}$ |
| $S_y$ | 0.301 | 0.223 | 0.389 |
| $a_c \ (m^{-1})$ | 5.68 | 3.81 | 12.61 |
| $a_k \ (m^{-1})$ | 23.66 | 6.32 | 44.31 |
| $\psi_a - \psi_k \ (cm)$ | 3.12 | 0.02 | 27.91 |
| $\log_{10}(C_{wD})$ | 3.44 | 2.83 | 4.12 |

Table 2: Comparison between parameter estimates obtained in this study on the basis of 11 transducer-measured drawdown records at Borden, those obtained based on the same records by *Endres et.al.* [2007] and on all measured drawdowns by *Moench* [2008].

| Parameters | ***Endres et.al.* [2007]** | ***Moench* [2008]** | **This study** |
|---|---|---|---|
| $K_r \ (m/s)$ | 6.10 × 10−5 | $6.84 \times 10^{-5}$ | 6.37 × 10−5 |
| $K_z \ (m/s)$ | 3.24 × 10−5 | 2.90 × 10−5 | 2.84 × 10−5 |
| $S_s \ (m^{-1})$ | 7.19 × 10−5 | 3.76 ×10−5 | 5.67 × 10−5 |
| $S_y$ | 0.284 | 0.25* | 0.301 |
| $a_c \ (m^{-1})$ | - | 5 | 5.68 |
| $a_k \ (m^{-1})$ | - | 31.7 | 23.66 |
| $\psi_a - \psi_k \ (cm)$ | - | - | 3.12 |

*Assigned (not estimated)

## FIGURE CAPTIONS

Figure 1. Schematic representation of system geometry.

Figure 2. Dimensionless drawdown $s_D = s_{CD} + s_{UD}$ versus dimensionless time $t_s$ in pumping well when $K_D = 1$, $S_s b/S_y = 1/100$, $a_{kD} = a_{cD} = 10$, $\psi_{aD} = \psi_{kD}$, $d_D = 0$, $l_D = 0.5$ and $C_{wD} = 1\text{x}10^2$. Also shown are confined component of our solution, $s_{cD}$, and solutions due to *Mishra and Neuman* [2010] and *Hantush* [1964].

Figure 3. Dimensionless drawdown versus dimensionless time in pumping well when $K_D = 1$, $S_s b / S_y = 1/100$, $a_{kD} = a_{cD} = 10$, $\psi_{aD} = \psi_{kD}$, $d_D = 0.0$, $l_D = 0.5$ for a range of $C_{wD}$ values. Also shown are solutions due to *Mishra and Neuman* [2010], *Hantush* [1964] and *Young et al.* [2006].

Figure 4. Dimensionless drawdown versus dimensionless time at $r_D = 0.2$ and $z_D = 0.5$ in saturated zone when $K_D = 1$, $S_s b / S_y = 1/100$, $a_{kD} = a_{cD} = 10$, $\psi_{aD} = \psi_{kD}$, $d_D = 0.0$, $l_D = 0.5$, $C_{wD}$ varies and $t_{Bs} = 0$. Also shown are solutions of *Mishra and Neuman* [2010] and *Hantush* [1964].

Figure 5. Dimensionless drawdown versus dimensionless time at $r_D = 0.2$ and $z_D = 0.5$ in saturated zone when $K_D = 1$, $S_s b / S_y = 1/100$, $a_{kD} = a_{cD} = 10$, $\psi_{aD} = \psi_{kD}$, $d_D = 0.0$, $l_D = 0.5$, $C_{wD} = 0$ and $t_{Bs}$ varies. Also shown is solution of *Mishra and Neuman* [2010].

Figure 6. Dimensionless drawdown versus dimensionless time at $r_D = 0.2$ and $z_D = 1.25$ in unsaturated zone when $K_D = 1$, $S_s b / S_y = 1/100$, $a_{kD} = a_{cD} = 10$, $\psi_{aD} = \psi_{kD}$, $d_D = 0.0$, $l_D = 0.5$, $C_{wD}$ varies and $t_{Bs} = 0$. Also shown is solutions of *Mishra and Neuman* [2010].

Figure 7. Drawdowns as functions of time computed analytically (solid) and numerically with STOMP (symbols) for synthetic pumping test at $r$ = 0.26, 0.80 and 1.51 m and $z = 2.0$ m in saturated zone.

Figure 8. Time-drawdowns at radial distance $r = 1.51$ m and elevation $z = 2.0$ m in saturated zone obtained (1) analytically with our solution and numerically with STOMP upon setting $C_{wD} = 58.2$ and $t_B$ = 0 min, and (2) analytically with the solution of *Mishra and Neuman* [2010] upon setting $t_B$ = 0.011 min.

Figure 9. Drawdowns as functions of time computed analytically (solid) and numerically with STOMP (symbols) for synthetic pumping test at $r$ = 1.51, 5.04 and 10.71 m and $z = 6.61$ m in unsaturated zone.

Figure 10. Plan view of pumping well PW1, piezometers and neutron access tubes at Borden. After *Moench* [2008].

Figure 11. Vertical view of initial water table, pumped well screen (dashed vertical line at the bottom of PW1), piezometers and neutron access tubes at Borden. After *Moench* [2008].

Figure 12. Simultaneous least squares fit of analytical solution (solid) to 11 water level records (symbols) at Borden measured by means of transducers.

Figure 13. Least squares fit between exponential constitutive models with parameters $a_c = 5.68\ m^{-1}$, $a_k = 23.66\ m^{-1}$ and $\psi_a - \psi_k = 3.12\ cm$ and *van Genuchten* [1980] - *Mualem* [1976] model with parameters $\psi_a = 34.1\ cm$, $\psi_k = 30.98\ cm$, $\alpha = 2.32\ m^{-1}$ and $n = 5.85$. Also shown are effective saturations based on measured initial static water content profile above water table in neutron access tube MBN − 5.

Figure 14. Predicted (solid) versus hand-measured (symbols) drawdowns in 14 piezometers not used in parameter estimation.

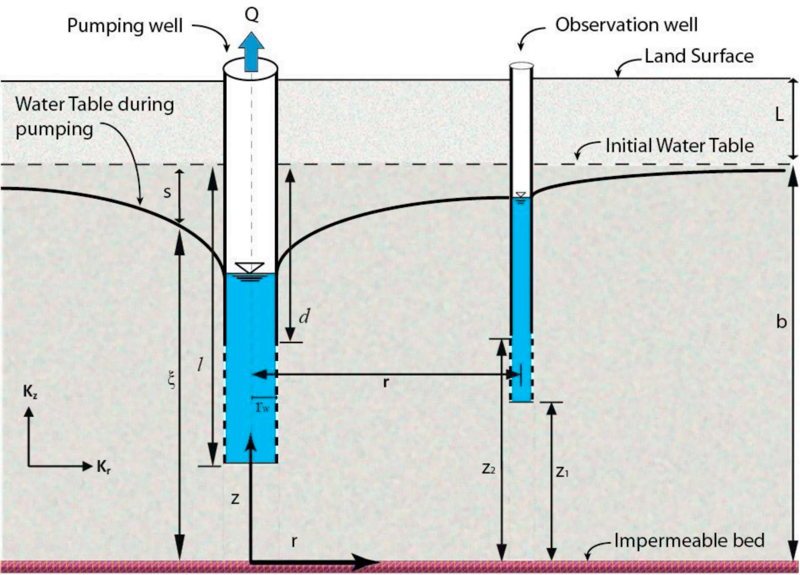

Q
Pumping well
Observation well
Land Surface
Water Table during pumping
L
Initial Water Table
s
d
b
l
ξ
r
$r_w$
$K_z$
$K_r$
$z_2$
$z_1$
z
r
Impermeable bed

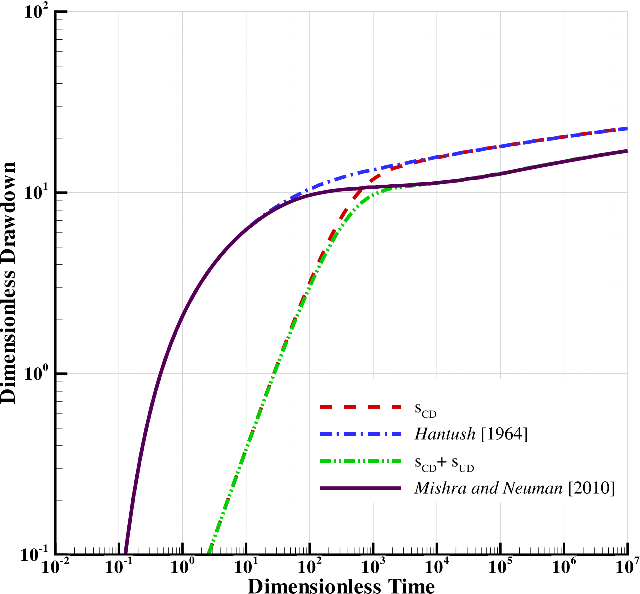

$10^2$
$10^1$
$10^0$
$10^{-1}$
Dimensionless Drawdown
$10^{-2}$
$10^{-1}$
$10^0$
$10^1$
$10^2$
$10^3$
$10^4$
$10^5$
$10^6$
$10^7$
Dimensionless Time
$s_{CD}$
*Hantush* [1964]
$s_{CD}+s_{UD}$
*Mishra and Neuman* [2010]

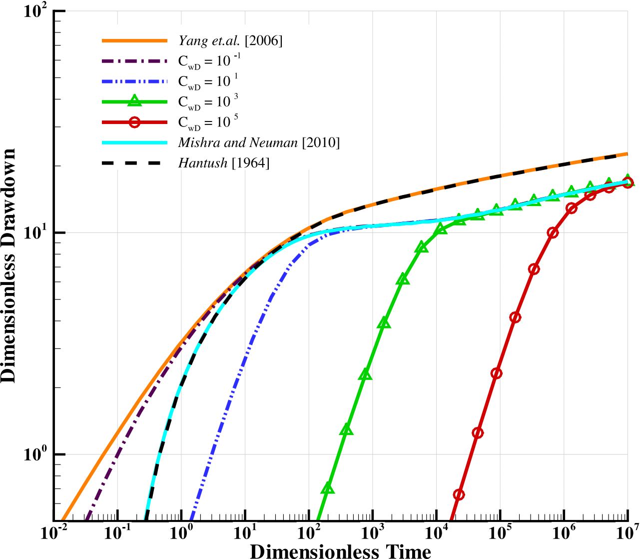

Yang et.al. [2006]
$C_{wD} = 10^{-1}$
$C_{wD} = 10^{1}$
$C_{wD} = 10^{3}$
$C_{wD} = 10^{5}$
Mishra and Neuman [2010]
Hantush [1964]
Dimensionless Drawdown
Dimensionless Time
$10^{-2}$
$10^{-1}$
$10^{0}$
$10^{1}$
$10^{2}$
$10^{3}$
$10^{4}$
$10^{5}$
$10^{6}$
$10^{7}$

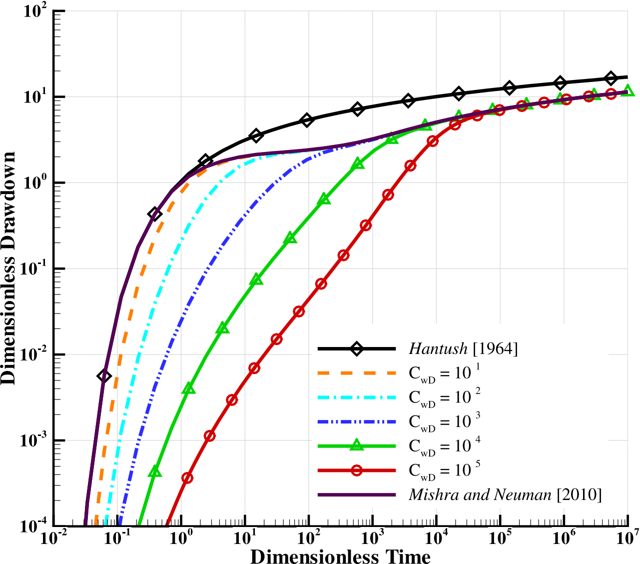

Dimensionless Drawdown
Dimensionless Time
$10^{-4}$
$10^{-3}$
$10^{-2}$
$10^{-1}$
$10^{0}$
$10^{1}$
$10^{2}$
$10^{-2}$
$10^{-1}$
$10^{0}$
$10^{1}$
$10^{2}$
$10^{3}$
$10^{4}$
$10^{5}$
$10^{6}$
$10^{7}$
*Hantush* [1964]
$C_{wD} = 10^{1}$
$C_{wD} = 10^{2}$
$C_{wD} = 10^{3}$
$C_{wD} = 10^{4}$
$C_{wD} = 10^{5}$
*Mishra and Neuman* [2010]

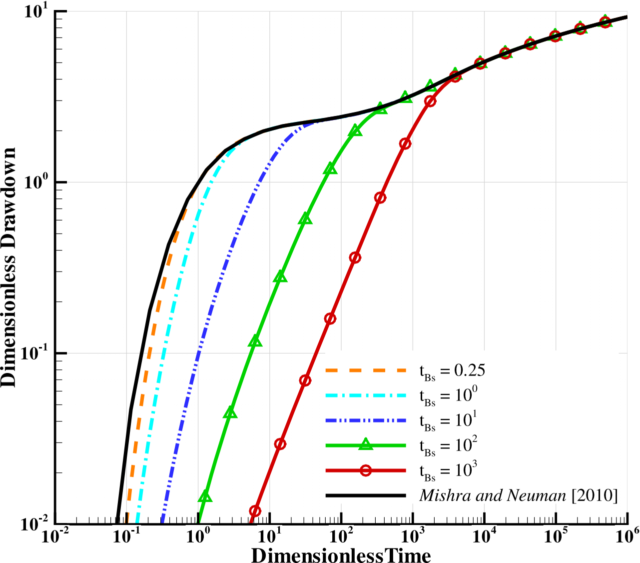

Dimensionless Drawdown
DimensionlessTime
$10^{1}$
$10^{0}$
$10^{-1}$
$10^{-2}$
$10^{-2}$
$10^{-1}$
$10^{0}$
$10^{1}$
$10^{2}$
$10^{3}$
$10^{4}$
$10^{5}$
$10^{6}$
$t_{Bs} = 0.25$
$t_{Bs} = 10^{0}$
$t_{Bs} = 10^{1}$
$t_{Bs} = 10^{2}$
$t_{Bs} = 10^{3}$
*Mishra and Neuman* [2010]

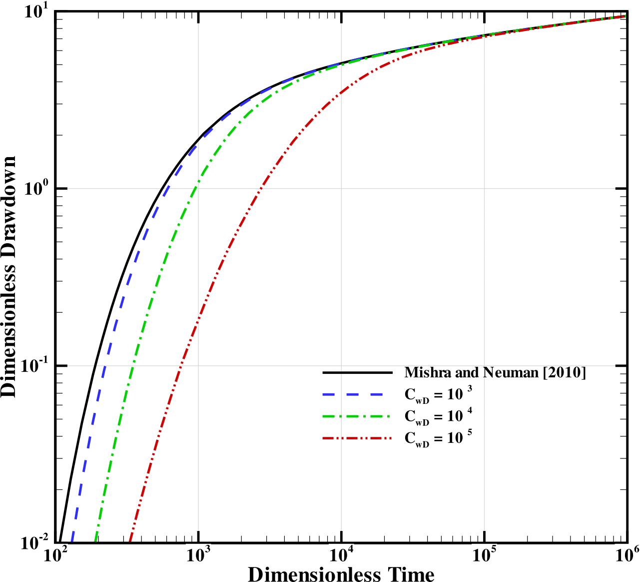

Dimensionless Drawdown
Dimensionless Time
$10^{1}$
$10^{0}$
$10^{-1}$
$10^{-2}$
$10^{2}$
$10^{3}$
$10^{4}$
$10^{5}$
$10^{6}$
Mishra and Neuman [2010]
$C_{wD} = 10^{3}$
$C_{wD} = 10^{4}$
$C_{wD} = 10^{5}$

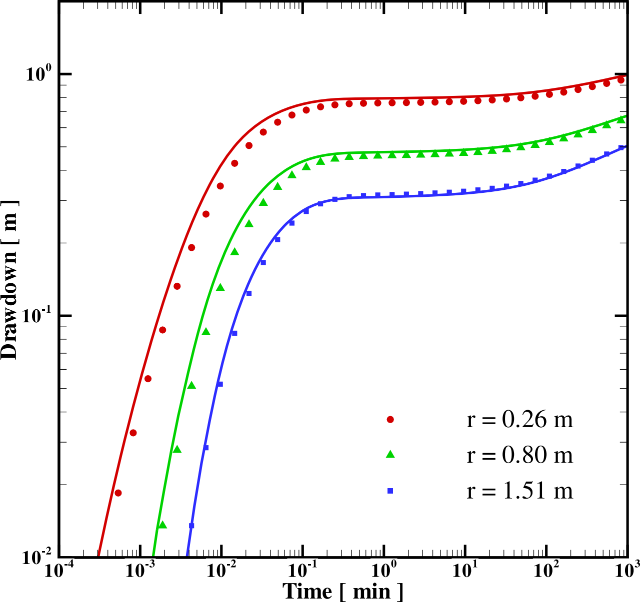

Drawdown [ m ]
Time [ min ]
$10^0$
$10^{-1}$
$10^{-2}$
$10^{-4}$
$10^{-3}$
$10^{-2}$
$10^{-1}$
$10^0$
$10^1$
$10^2$
$10^3$
r = 0.26 m
r = 0.80 m
r = 1.51 m

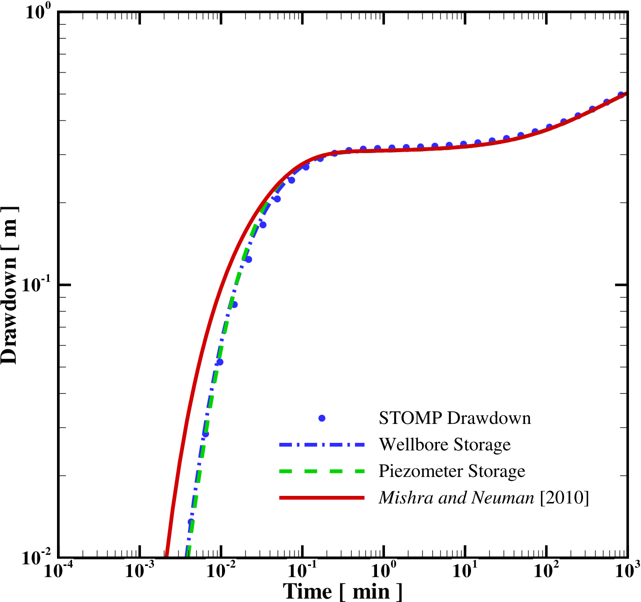

Drawdown [ m ]
Time [ min ]
$10^{0}$
$10^{-1}$
$10^{-2}$
$10^{-4}$
$10^{-3}$
$10^{-2}$
$10^{-1}$
$10^{0}$
$10^{1}$
$10^{2}$
$10^{3}$
STOMP Drawdown
Wellbore Storage
Piezometer Storage
*Mishra and Neuman* [2010]

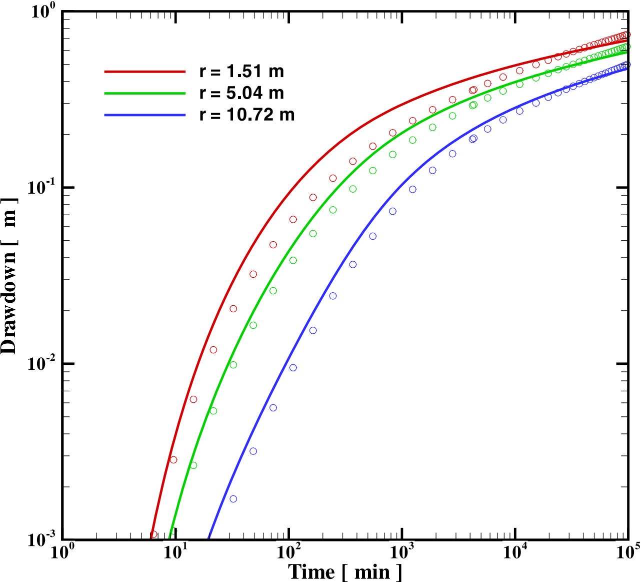

r = 1.51 m
r = 5.04 m
r = 10.72 m
Drawdown [ m ]
Time [ min ]
$10^0$
$10^{-1}$
$10^{-2}$
$10^{-3}$
$10^0$
$10^1$
$10^2$
$10^3$
$10^4$
$10^5$

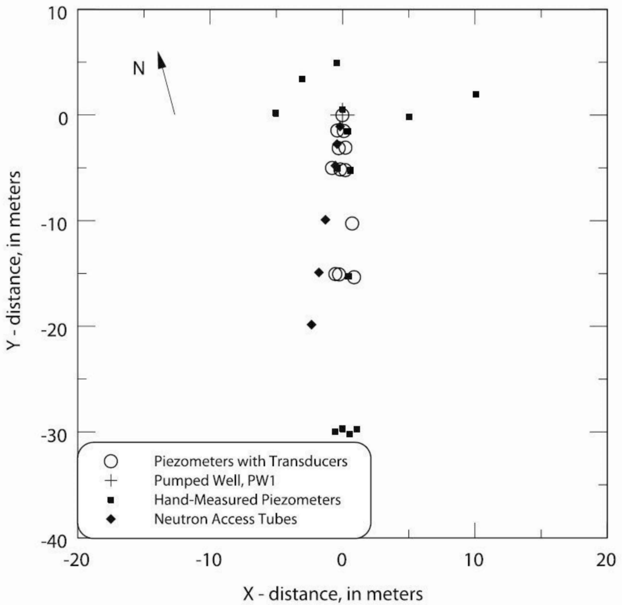

10
0
-10
-20
-30
-40
-20
-10
0
10
20
N
Y - distance, in meters
X - distance, in meters
Piezometers with Transducers
Pumped Well, PW1
Hand-Measured Piezometers
Neutron Access Tubes

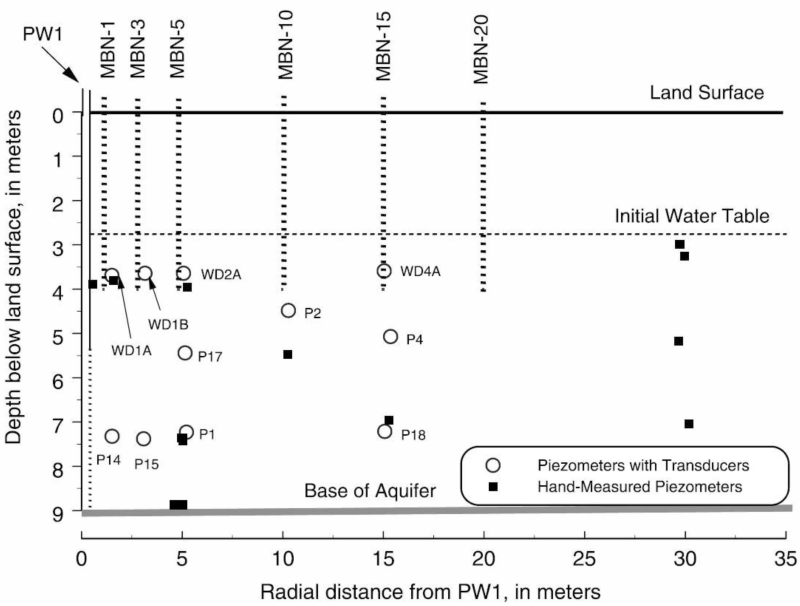
PW1
MBN-1
MBN-3
MBN-5
MBN-10
MBN-15
MBN-20
Land Surface
Initial Water Table
WD2A
WD4A
WD1B
WD1A
P2
P4
P17
P1
P18
P14
P15
Base of Aquifer
Piezometers with Transducers
Hand-Measured Piezometers
Depth below land surface, in meters
0
1
2
3
4
5
6
7
8
9
0
5
10
15
20
25
30
35
Radial distance from PW1, in meters

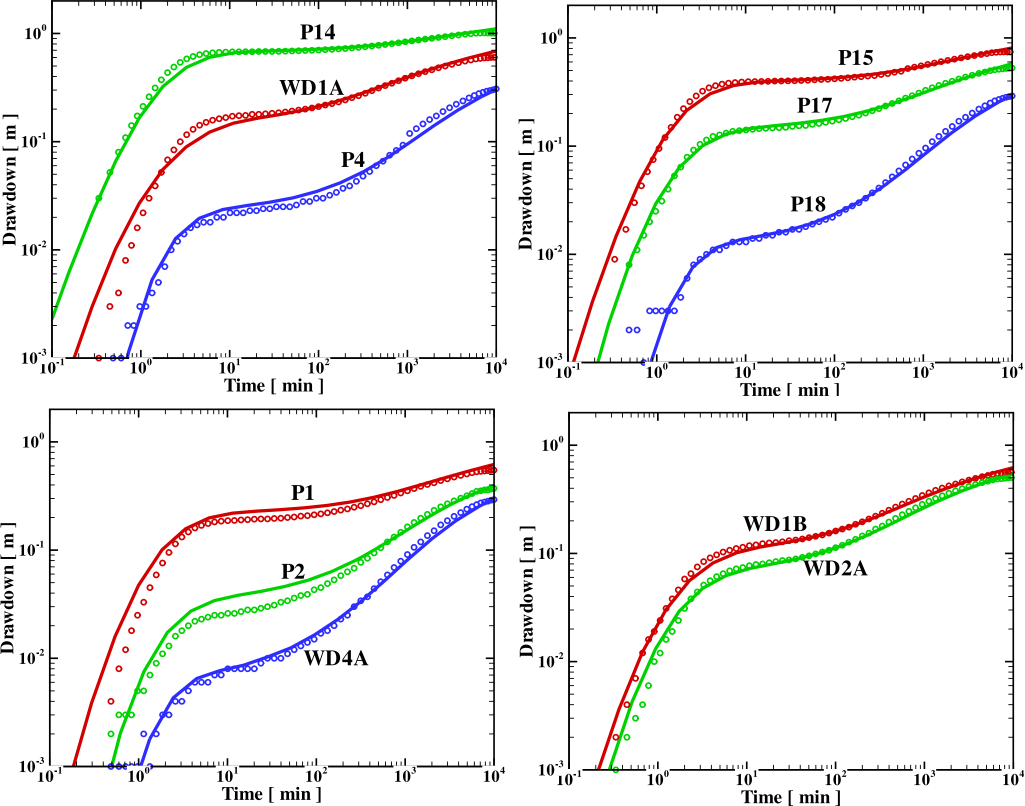

P14
WD1A
P4
Drawdown [ m ]
Time [ min ]
P15
P17
P18
Drawdown [ m ]
Time [ min ]
P1
P2
WD4A
Drawdown [ m ]
Time [ min ]
WD1B
WD2A
Drawdown [ m ]
Time [ min ]

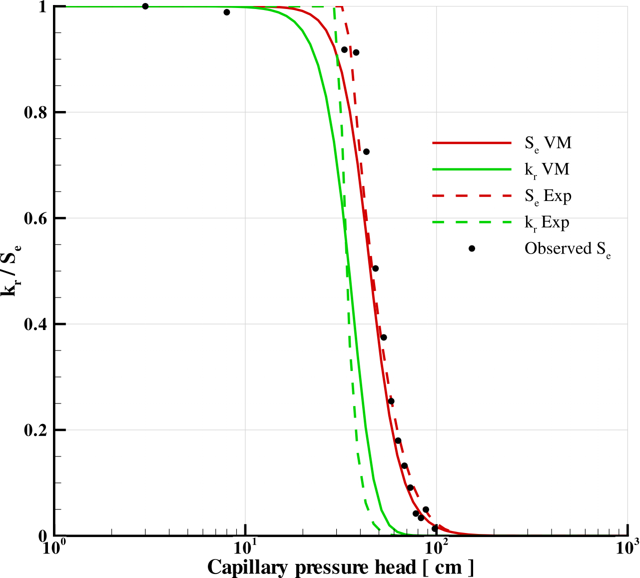

$S_e$ VM
$k_r$ VM
$S_e$ Exp
$k_r$ Exp
Observed $S_e$
$k_r$ / $S_e$
Capillary pressure head [ cm ]
0
0.2
0.4
0.6
0.8
1
$10^0$
$10^1$
$10^2$
$10^3$

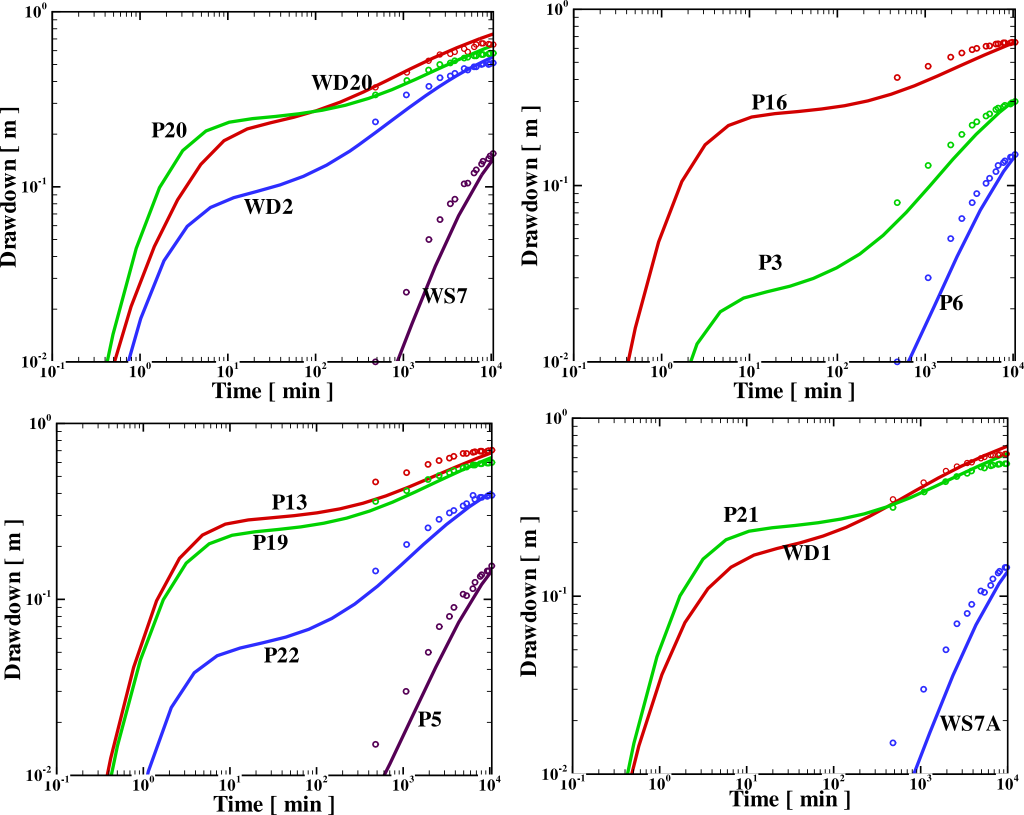

Drawdown [ m ]
Time [ min ]
WD20
P20
WD2
WS7
P16
P3
P6
P13
P19
P22
P5
P21
WD1
WS7A